Band structure and optical response of 2*H*-MoX_2 compounds (X=S, Se, and Te)

Ali Hussain Reshak and Sushil Auluck
Physics Department, Indian Institute of Technology, Roorkee (Uttaranchal) 247667, India
(Received 24 September 2004; revised manuscript received 29 November 2004; published 19 April 2005)

We report calculations of the electronic and optical properties for the 2*H*-MoX_2 (X=S, Se, Te) compounds using the full potential linear augmented plane wave method within the local density approximation. When S is replaced by Se and Te, the energy gap changes and the bandwidth of the Mo-*d* bands reduces. From the partial density of states we find a strong hybridization between Mo-*d* and *X*-*p* states below the Fermi energy E_F. On going from S to Se to Te the structures in the frequency-dependent imaginary part of the dielectric function $\varepsilon_2(\omega)$ shifts towards lower energies. The frequency-dependent reflectivity and absorption show that the plasma minimum also shifts towards lower energies. We compare our calculations with the experimental optical data and find a good agreement.

DOI: 10.1103/PhysRevB.71.155114 PACS number(s): 71.15.Ap

I. INTRODUCTION

2*H*-MoX_2 (X=S, Se and Te) compounds are interesting members of the transition metal dichalcogenide compounds (TMDC's). These compounds are used for electrodes in high-efficiency photoelectrochemical (PEC) cells.[1] As the phototransitions involve nonbonding *d* orbitals of Mo atoms, these compounds can be expected to resist hole-induced corrosion.[2] Studies have shown that the texture of thin films of these compounds is an important factor for their photoactivity. The (001) texture is favorable for application in solar cells because such films have low surface states and hence fewer charge-carrier recombination centers.[3] 2*H*-MoX_2 compounds are known to be extremely good solid lubricants, and they present ideal surfaces on which to carry out absorption. In addition to this they can also act as catalysts. These compounds have highly anisotropic physical properties. Hence they can be intercalated with foreign atoms. The intercalation of lithium in MoS_2 (Refs. 4–7) has led to its use in lithium batteries.

Santiago *et al.*[8] synthesized MoS_2 nanotubes with diameters greater than 10 nm, using the template method. Zheng *et al.*[9] applied a simple ultrasound-assisted cracking process to prepare high-crystallinity 2*H*-MoS_2 nanorods using MoS_2 micron particles as raw materials. Rettenberger *et al.*[10] used femtosecond laser photoemission to investigate the electron dynamics in the layered semiconductor 2*H*-$MoSe_2$.

Optical absorption measurements and reflection spectroscopy have been performed on 2*H*-MoX_2 (Refs. 11–17) compounds. Beal *et al.*[13] measured the transmission spectra of 2*H*-MoX_2 compounds in the energy range of 0–4.0 eV for the electric field $\vec{E} \perp \mathbf{c}$. Liang[16] measured the reflectivity spectra using polarized light with $\vec{E} \perp \mathbf{c}$ as well as $\vec{E} \parallel \mathbf{c}$, in the energy range between 0 and 5.0 eV for 2*H*-$MoTe_2$. Hughes and Liang[17] measured the vacuum ultraviolet reflectivity spectra of 2*H*-MoX_2 compounds in the range of 4.5–14 eV for $\vec{E} \perp \mathbf{c}$. Beal and Hughes[14] measured the reflectivity spectrum of 2*H*-MoX_2 for $\vec{E} \perp \mathbf{c}$. Amirtharaj *et al.*[12] reported an electrolyte electroreflectance (EER) study of 2*H*-$MoSe_2$ in the energy range of 0.7–6 eV.

The physical and structural properties of 2*H*-MoX_2 compounds have been reviewed extensively by Wilson and Yoffe.[11] There is some disagreement regarding the magnitude of the energy gap in 2*H*-MoS_2. Wilson and Yoffe attributed a weak indirect edge of 0.2 eV to the semiconducting energy gap. Huisman and Jellinek[18] believe that this 0.2 eV structure is extrinsic and proposed that the intrinsic gap is ~1.4 eV. Mattheiss[19] calculated the electronic band structure of 2*H*-MoS_2 using the nonrelativisitic augmented plane wave (APW) method and found an indirect gap of about 1.16 eV. Coehoorn and co-workers[20,21] calculated the band structure of 2*H*-MoS_2/Se_2 using the augmented spherical wave (ASW) method. They conclude that the top of the valence band is situated at Γ, and the bottom of the conduction band is halfway between Γ and *K*, resulting in an indirect gap of 0.15 and 0.35 eV, respectively. Seifert *et al.*[22] studied the structural and electronic properties as well as the stability of 2*H*-MoS_2 nanotubes using a density-functional-based tight-binding method. Kobayashi and Yamauchi[23] calculated the band structure and the scanning tunneling microscopy (STM) images of 2*H*-MoS_2/Se_2 surfaces using the ultrasoft pseudopotential with the plane-wave (PW) basis and the linear combination of atomic orbitals (LCAO) methods. Boker *et al.*[24]

TABLE I. Lattice parameters and energy gaps for 2*H*-MoX_2 compounds.

	2*H*-MoS_2	2*H*-$MoSe_2$	2*H*-$MoTe_2$
a (Å)	3.160[a]	3.288[a]	3.518[b]
c (Å)	12.29[a]	12.90[a]	13.97[b]
z	0.621[a]	0.621[a]	0.621[b]
Exp E_g (eV)	1.29[c], 1.23[d]	1.1[c]	1.0[c]
Th. E_g (eV)	0.2[b], 1.45[e], 1.15[g], 0.15[e], 0.77[i], 0.7[i]	0.35[e] 0.75[h]	0.7[f] 0.55[h]

[a]Refs. 11 and 19.
[b]Ref. 11.
[c]Ref. 24.
[d]Refs. 31 and 32.
[e]Refs. 18, 20, and 21.
[f]Ref. 26.
[g]Ref. 19.
[h]This work.
[i]Ref. 23.

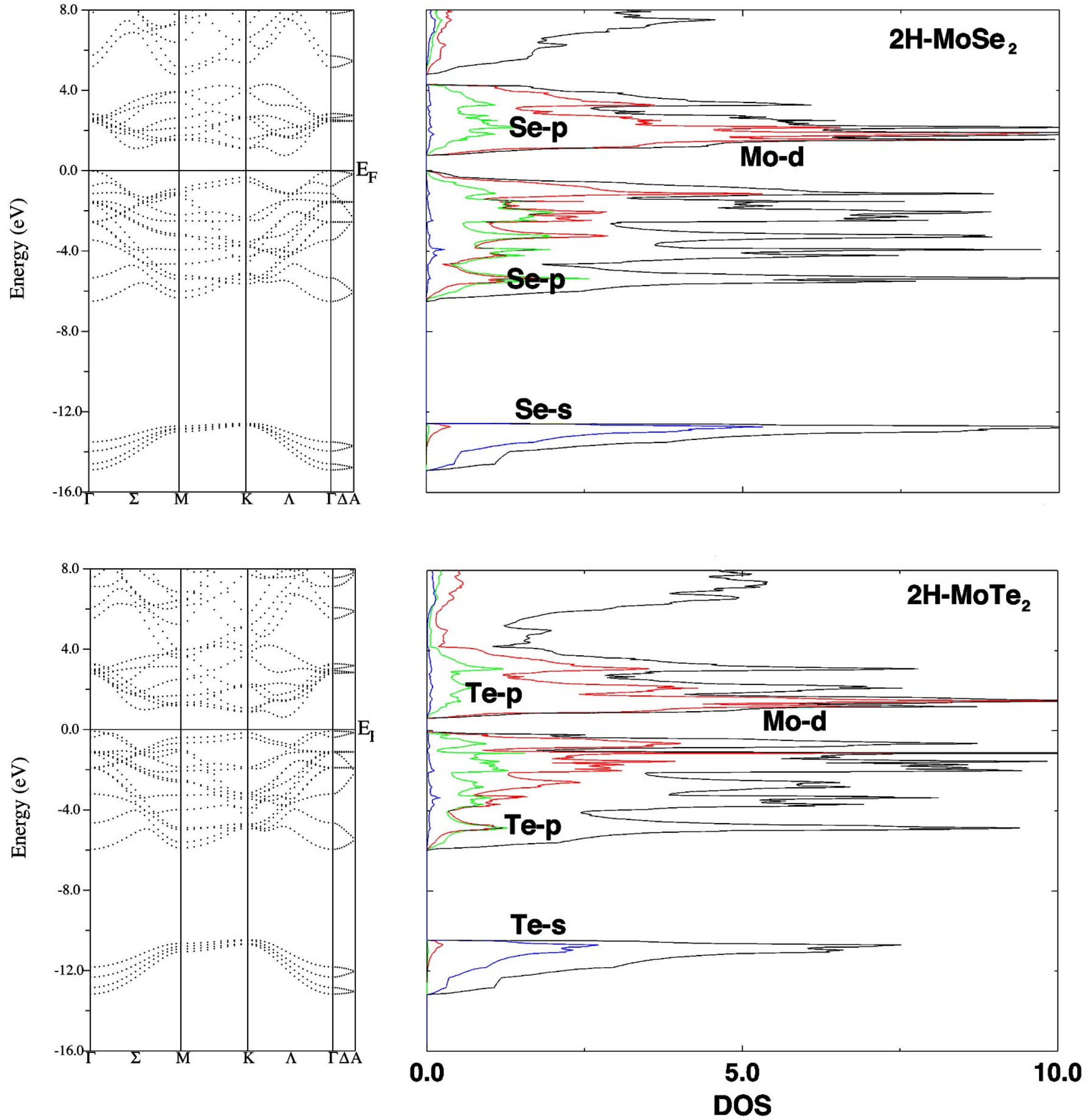

FIG. 1. Band structure and total DOS (—) in states/eV unit cell, along with the partial DOS, where (· · ·) denotes chalcogen-*s*, (· · ·)), and (· · ·) Mo-*d* states for $2H$-$MoSe_2$ and $2H$-$MoTe_2$. All the partial DOS are multiplied by 3.

presented the valence band structure of $2H$-MoX_2 compounds using both angle-resolved photoelectron spectroscopy (ARPES) with synchrotron radiation, as well as *ab initio* band-structure calculations. Boker *et al.*[25] presented a complete band structure of $2H$-$MoTe_2$ using ARPES with synchrotron radiation. Dawson and Bullett[26] calculated the electronic structure of $2H$-$MoTe_2$ using the *ab inito* LCAO method. Hindt and Lee[27] used the Korringa-Kohn-Rostoker (KKR) method to calculate the electronic band structure for $2H$-$MoTe_2$. All of the above calculations showed that the valence- band maximum (VBM) is located at Γ. Dawson and Bullett[26] showed the VBM at *M* for $2H$-$MoTe_2$. The PW calculations of Kobayashi and Yamauchi[23] found the conduction-band minimum (CBM) at Γ. All other calculations yielded the CBM between Γ and *K*.

There exist many band-structure calculations for the $2H$-MoX_2 compounds. However, most of these calculations are based on the muffin tin approximation, which is known to be a poor approximation for the layered structure materials. These calculations show a large variation in the energy gaps (Table I) and discrepancies in the VBM and CBM locations. We have therefore, perform calculations using the full potential method to throw light on these discrepancies. Even though there exist many measurements of the optical properties for the $2H$-MoX_2 compounds, there seems to be a dearth of theoretical calculations. We present detailed calculations of the optical properties of the $2H$-MoX_2 compounds with the intent to compare them with the experimental data.

In Sec. II we give the details of our calculations. The band structure and density of state are presented and discussed in Sec. III. The frequency-dependent dielectric function and other optical properties are given in Sec. IV, and Sec. V summarizes our conclusions.

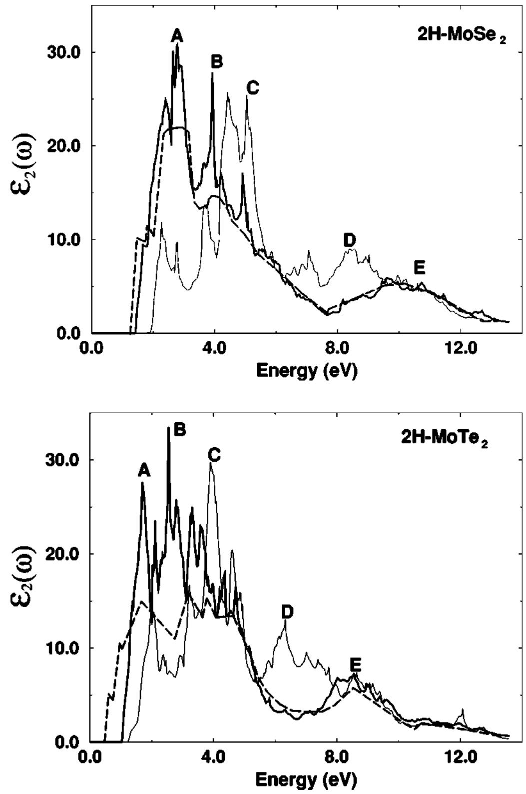

FIG. 2. Calculated $\varepsilon_2^{\perp}(\omega)$ (—) and $\varepsilon_2^{\parallel}(\omega)$ (—) along with the $\varepsilon_2^{\perp}(\omega)$ experimental data (- - -) of Beal and Hughes (Ref. 14) for 2*H*-$MoSe_2$ and 2*H*-$MoTe_2$.

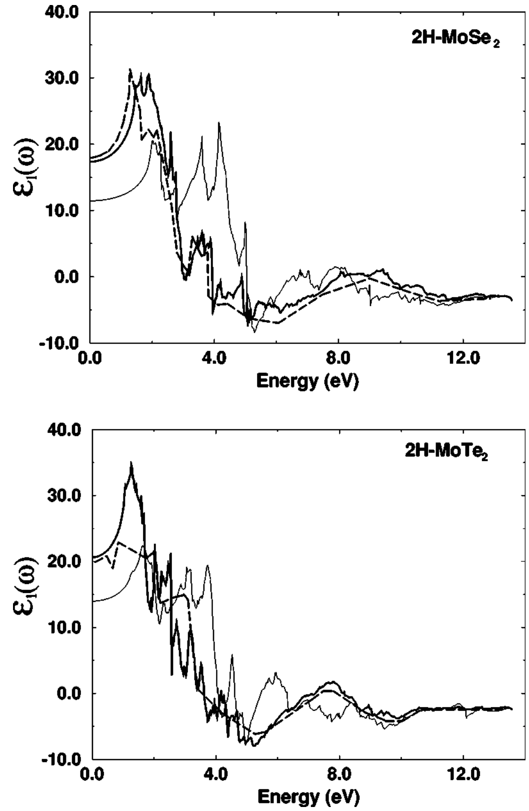

FIG. 3. Calculated $\varepsilon_1^{\perp}(\omega)$ (—) and $\varepsilon_1^{\parallel}(\omega)$ (—) along with the $\varepsilon_1^{\perp}(\omega)$ experimental data (· · ·) of Beal and Hughes (Ref. 14) for 2*H*-$MoSe_2$ and 2*H*-$MoTe_2$.

II. METHOD OF CALCULATION

In our work we use the full potential linear augmented plane wave (FPLAPW) method as incorporated in the WIEN97 code.[28] The exchange-correlation (XC) potential is constructed following von Barth and Hedin.[29] 2*H*-MoX_2 crystallizes in a hexagonal structure with space group $[P6_3/mmc(D_{6h}^4)]$. The two equivalent Mo atoms are located at $2c$ sites $\pm(1/3,2/3,1/4)$ and the four chalcogen atoms at $4f$ sites $\pm(1/3,2/3,z)$ and $\pm[2/3,1/3,(z+1/2)]$. The experimental lattice parameters are listed in Table I. Self-consistency is obtained using 200 *k* points in the irreducible Brillouin zone (IBZ), and the Brillouin zone (BZ) integrations are carried out using the tetrahedron method.[30] The density of states, band structures, and frequency-dependent anisotropic optical properties are calculated using 500 *k* points in the IBZ.

TABLE II. The approximate location of the structures (in eV) shown in Fig. 2 and the values of calculated $\varepsilon_1(0)$.

	2*H*-MoS_2	2*H*-$MoSe_2$	2*H*-$MoTe_2$
A	3.0	2.8	1.8
B	4.5	3.9	2.2
C	5.5	5	3.9
D	9	8.5	6.2
E	10.5	10	8.5
$\varepsilon_1^{\perp}(0)$	16	17.5	20.5
$\varepsilon_1^{\parallel}(0)$	10	12	14
$\varepsilon_1^{\perp}(0)$ exp[a]	17.0	18.0	20.0

[a](Ref. 14)

III. RESULT AND DISCUSSION

Band structure and density of states

The band structure and the total density of states (DOS) along with the chalcogen-*s*, chalcogen-*p*, and Mo-*d* partial DOS for 2*H*-$MoSe_2$/Te_2 are shown in Fig. 1. As the 2*H*-MoS_2 calculations were published earlier,[7] we choose not to show them. Our calculations show that 2*H*-$MoSe_2$ and 2*H*-$MoTe_2$ are semiconductors with indirect energy gaps of 0.75 eV and 0.55 eV, respectively. The VBM is located at Γ and the CBM between Γ and K. From the partial DOS we are able to identify the angular momentum character of the various structures. The lowest four bands are mainly due to the chalcogen-*s* states. The bands in the energy range of −6 to −1 eV for 2*H*-$MoSe_2$ (−6.5 to −1 eV for 2*H*-$MoTe_2$) are mainly chalcogen-*p* states. Bands between −1 eV to the Fermi energy (E_F) and above it, between 0.7 and 4 eV (0.5 to 4 eV for 2*H*-$MoTe_2$), are mainly Mo-*d* states. The last structure from 4.5 eV and above is composed of chalcogen-*p* and Mo-*spd* states. The last two groups in 2*H*-$MoTe_2$ are merged. Our calculated band structures for 2*H*-MoS_2 (Ref. 7) and 2*H*-$MoSe_2$ are similar to the band

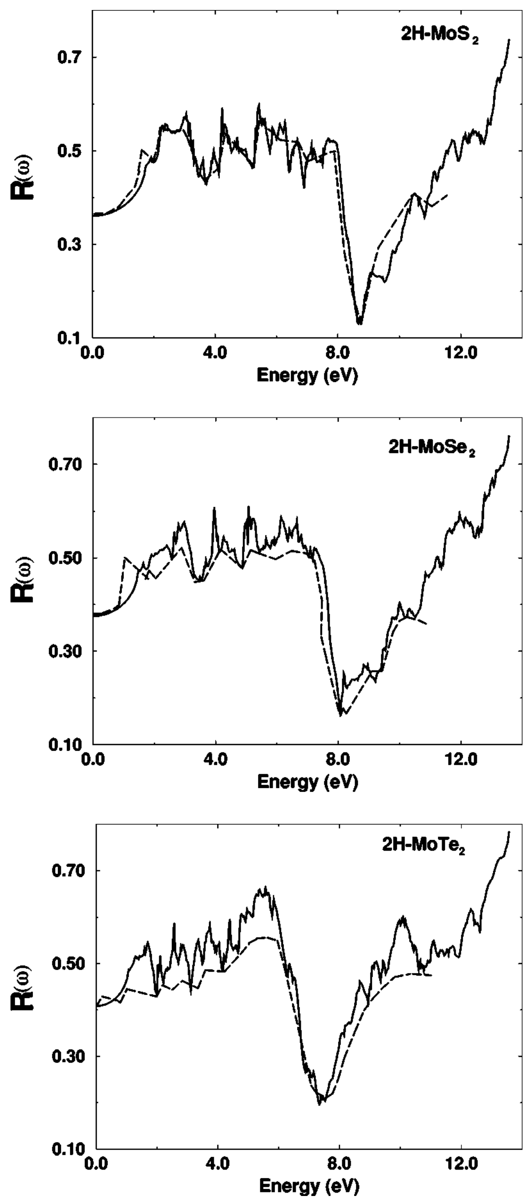

FIG. 4. Calculated reflectivity spectrum (—) for $\vec{E} \perp \mathbf{c}$ along with the experimental data (Refs. 14 and 17) (- - -) for 2*H*-MoX_2 compounds.

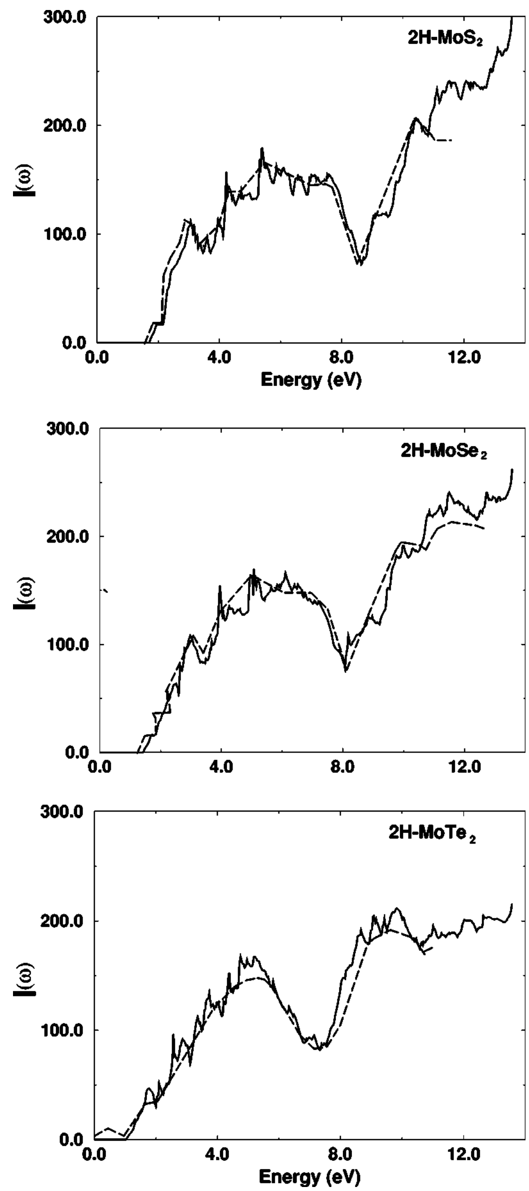

FIG. 5. Calculated absorption coefficient (—) for $\vec{E} \perp \mathbf{c}$ along with the experimental data (Ref. 14) (- - -) for the 2*H*-MoX_2 compounds.

structures obtained by the APW,[19] ASW,[20] ARPES,[25] and PW[23] methods and different from that obtained by the LCAO[23] method. The band structure for 2*H*-$MoTe_2$ is similar to that obtained by the ARPES[24,25] and KKK[27] methods and different from that obtained by the LCAO method,[26] in terms of VBM and CBM locations. In Table I, we compare our calculated energy gaps with those of the other calculations. We see that there are significant differences. This indicates the relevance of a full potential calculation. Our calculated energy gaps are always less then the measured energy gaps. This is consistent with the fact that local density approximation (LDA) is known to underestimate bands gaps[33] by around 40%. As we move from S to Se to Te the bandwidth of the Mo-*d* and chalcogen-*s* bands reduces and the Mo-*d* bands shift towards higher energies by around 0.5 eV with respect to E_F. The chalcogen-*s* bands shift to lower energies when we move from S to Se and to higher energies when we move from Se to Te. The S-*p* and Se-*p* states hybridize strongly with the Mo-*d* states below E_F, while the Te-*p* states shows less hybridization.

IV. OPTICAL PROPERTIES

Figure 2 shows the calculated $\varepsilon_2^{\perp}(\omega)$ and $\varepsilon_2^{\parallel}(\omega)$ for 2*H*-$MoSe_2/Te_2$. We find that the transitions from the chalcogen-*p* states (valence band) to the Mo-*d* states (conduction bands) are responsible for the structures in $\varepsilon_2(\omega)$. $\varepsilon_2^{\perp}(\omega)$ shows structures at *A*, *B*, and *E*, while $\varepsilon_2^{\parallel}(\omega)$ shows them at *C* and *D*. The location of these structures is listed in Table II. We note that the structures move towards lower energies as we go from S to Se to Te. Since only $\varepsilon_2^{\perp}(\omega)$ has been measured, we compare our calculated $\varepsilon_2^{\perp}(\omega)$ with the experimental data of Beal and Hughes,[14] and find a good agreement.

From the imaginary part of the dielectric functions the real part can be calculated by using Kramers-Kronig relations. We present $\varepsilon_1^{\perp}(\omega)$ and $\varepsilon_1^{\parallel}(\omega)$ for $2H$-$MoSe_2/Te_2$ along with the experimental data of Beal and Hughes[14] for $\varepsilon_1^{\perp}(\omega)$ in Fig. 3. The calculated values of $\varepsilon_1^{\perp}(0)$ and $\varepsilon_1^{\parallel}(0)$ are given in Table II. A good agreement is found with the experimental[14] values.

The calculated reflectivity spectra is shown in Fig. 4. It is immediately apparent that the gross features are very similar. This is due to the fact that the band structures for these compounds are indeed quite similar. We notice a strong reflectivity minimum that indicates a collective plasma resonance. The depth of the plasma minimum is determined by the imaginary part of the dielectric function at the plasma resonance, and it is representative of the degree of overlap between the interband absorption regions on either side of the energy window.[14,17] The plasma minimum shifts towards lower energies with increasing depth as we move from S to Se to Te. Our calculations show a very good agreement with the experimental data of Beal and Hughes[14] and Hughes and Liang.[17]

The frequency-dependent absorption coefficient is shown in Fig. 5. The plasma resonance, corresponding to the minima in the absorption coefficient, shifts towards lower energies when we move from S to Se to Te. We compare our calculated absorption coefficient with the experimental data of Beal and Hughes[14] and find an excellent agreement.

V. CONCLUSIONS

We have studied the electronic and optical properties of the $2H$-MoX_2 compounds with the intent to ascertain the effect of replacing S by Se and Te. When we moved from S to Se to Te the bandwidth of the Mo-*d* and chalcogen-*s* bands reduced and the Mo-*d* bands shifted towards higher energies. The chalcogen-*s* bands shifted towards lower energies when S was replaced by Se and towards higher energies when Se was replaced by Te. All the compounds showed four groups and/or structures in the band structure and DOS corresponding to the chalcogen-*s*, chalcogen-*p*, and Mo-*d* states and Mo-*spd* and chalcogen-*p* states. There is a strong hybridization between chalcogen-*p* and Mo-*d* states below E_F in $2H$-MoS_2 and $2H$-$MoSe_2$, while in $2H$-$MoTe_2$ it is weak. Our calculated band structure and DOS showed a better agreement with the experimental work than some of the earlier calculations in the matters of the energy-gap values[11,19,20,23] and VBM and CBM locations.[23,26] The frequency-dependent optical properties showed that the structures in the dielectric function moved towards lower energies on going from S to Se to Te. In the reflectivity spectrum and the absorption coefficient the plasma frequency minimum shifted towards lower energies with increased depth. An excellent agreement is found with the experimental data.

ACKNOWLEDGMENTS

We would like to thank the Institute Computer Center and Physics Department for providing the computational facilities.

[1] H. D. Abruna, G. A. Hope, and A. J. Bard, J. Electrochem. Soc. **129**, 2224 (1982).
[2] M. Kettaf, A. Conan, A. Bonnet, and J. C. Bernede, J. Phys. Chem. Solids **51**, 333 (1990).
[3] Helmut Tributsch, Solar Energy Research (HMI Annual Report 2002) p. 89.
[4] X. Rocquefelte, F. Boucher, P. Gressier, G. Ouvrard, P. Blaha, and K. Schwarz, Phys. Rev. B **62**, 2397 (2000).
[5] V. Petkov, S. J. L. Billinge, P. Larson, S. D. Mahanti, T. Vogt, K. K. Rangan, and M. G. Kanatzidis, Phys. Rev. B **65**, 092105 (2002).
[6] Ali Hussain Reshak, S. Auluck, and S. Sharma, International Conference on High Pressure and Technology, (N.P.L., New Delhi, India, 2001), p. 194.
[7] Ali Hussain Reshak and S. Auluck, Phys. Rev. B **68**, 125101 (2003).
[8] P. Santiago, J. A. Ascencio, D. Mendoza, M. Perez-Alvarez, A. Espinosa, C. Reza-Sangerman, P. Schabes-Retchkiman, G. A. Camacho-Bragado, and M. Jose-Yacaman, Appl. Phys. A: Mater. Sci. Process. **78**, 513 (2004).
[9] Zheng Xiuwen, Zhu Liying, Yan Aihui, Bai Chuannan, Xie Yi, Ultrason. Sonochem. **11**, 83 (2004).
[10] A. Rettenberger, P. Leiderer, M. Probst, and R. Haight, Phys. Rev. B **56**, 12 092 (1997).
[11] J. A. Wilson and A. D. Yoffe, Adv. Phys. **18**, 193 (1969).
[12] P. M. Amritraj, F. H. Pollak, and A. Wold, Solid State Commun. **41**, 581 (1982).
[13] A. R. Beal, J. C. Knights, and W. Y. Liang, J. Phys. C **5**, 3540 (1972).
[14] A. R. Beal and H. P. Hughes, J. Phys. C **12**, 881 (1979).
[15] M. G. Bell and W. Y. Liang, Adv. Phys. **25**, 52 (1976).
[16] W. Y. Liang, J. Phys. C **6**, 551 (1973).
[17] H. P. Hughes and W. Y. Liang, J. Phys. C **7**, 1023 (1974).
[18] R. Huisman and F. J. Jellinek, J. Less-Common Met. **17**, 111 (1969).
[19] L. F. Mattheiss, Phys. Rev. B **8**, 3719 (1973).
[20] R. Coehoorn, C. Hass, J. Dijikstra, C. J. F. Flipse, R. A. De Groot, and A. Wold, Phys. Rev. B **35**, 6195 (1987).
[21] R. Coehoorn, C. Hass, R. A. De Groot, and A. Wold, Phys. Rev. B **35**, 6203 (1987).
[22] G. Seifert, H. Terrones, M. Terrones, G. Jungnicket, and T. Frauenheim, Phys. Rev. Lett. **85**, 146 (2000).
[23] Katsuyoshi Kobayashi and Jun Yamauchi, Phys. Rev. B **51**, 17 085 (1995).
[24] Th. Boker, R. Severin, A. Muller, C. Janowitz, R. Manzke, D. VoB, P. Kruger, A. Mazur, and J. Pollmann, Phys. Rev. B **64**, 235305 (2001).
[25] Th. Boker, A. Muller, J. Augustin, C. Janowitz, and R. Manzke, Phys. Rev. B **60**, 4675 (1999).
[26] W. G. Dawson and D. W. Bullett, J. Phys. C **20**, 6159 (1987).

[27] S. P. Hindt and P. M. Lee, J. Phys. C **13**, 349 (1980).
[28] P. Blaha, K. Schwarz, and J. Luitz, WIEN97, Vienna University of Technology, 1997 (improved and updated unix version of the original copywright WIEN Code) which was published by P. Blaha, K. Schwartz, P. Sorantin, and S. B. Trickey, Comput. Phys. Commun.59, 399 (1990).
[29] U. von Barth, and L. Hedin, J. Phys. C **5**, 1629 (1972).
[30] O. Jepsen and O. K. Andersen, Solid State Commun. **9**, 1763 (1971); G. Lehmann and M. Taut, Phys. Status Solidi B **54**, 496 (1972).
[31] K. K. Kam and B. Parkinson, J. Phys. Chem. **86**, 463 (1982).
[32] K. K. Kam, C. L. Chang, and D. W. Lynch, J. Phys. C **17**, 4031 (1984).
[33] S. N. Rashkeev, W. R. L. Lambrecht, and B. Segall, Phys. Rev. B **57**, 3905 (1998).